The Influence of Stratospheric Ozone Concentrations on the General Atmospheric Circulation of an Aquaplanet

Nick Androski

December 9, 2024

1 Introduction

Stratospheric ozone, despite it's relatively small concentration compared to other gases in the atmosphere, has a large influence on the climate on Earth. Ozone in the stratosphere is primarily responsible for the existence of a tropopause, where lapse rate of temperature switches sign and separates the unstably stratified troposphere from the stably stratified stratosphere.
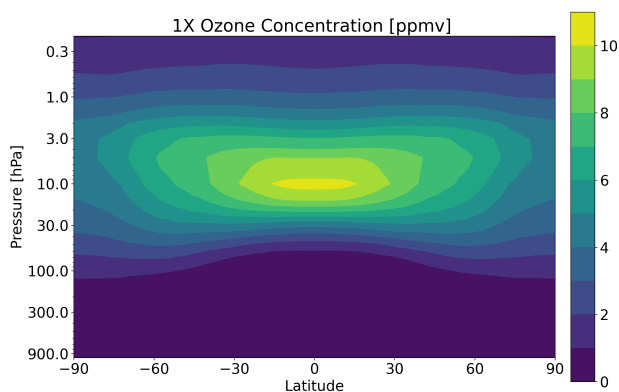

Figure 1: Zonally uniform ozone distribution for the 1×O3 control run based upon the AquaPlanet Experiment project specifications created by an annual average of the monthly AMIP ozone climatology.

Ozone in the stratosphere is in a photochemical equilibrium created by a balance between ozone production and destruction. First, a UV rays split molecular oxygen (O2) into oxygen atoms. Then, these oxygen atoms combine with molecular oxygen in the atmosphere to form ozone. The ozone reacts continuously with UV sunlight that split it apart. Additionally, ozone is a highly reactive gas and can react with many trace gases in the atmosphere, such as chlorofluorocarbon (CFC) which caused the ozone hole. The net result is a distribution of ozone that is most concentrated at the tropics and smallest at the poles, following this distribution of solar insolation on Earth. See Fig. 1 for a typical ozone concentration on Earth. In reality, this distribution changes seasonally as solar insolation varies over Earth.

The formation and destruction process of ozone creates a continuum absorption band of UV radiation between around $200 - 300$ nm.
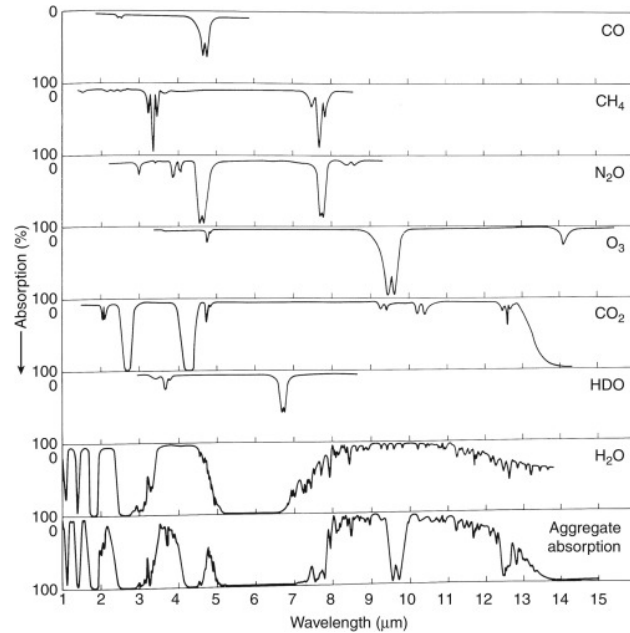

Figure 2: Infrared absorption spectrum for key molecules in Earth's atmosphere. Obtained from Figure 3.4 in Hartmann (2016b), created by Valley (1965).

Furthermore, ozone has several vibration-rotation absorption bands, including one at 9.6 μm in the infrared. This wavelength is particularly impactful because it lies in the atmospheric window, making ozone an effective greenhouse gas. The atmospheric window, shown in Fig. 2, is a region on the infrared spectrum between 8 to 13 μm where the atmosphere is relatively transparent due to a lack of molecules with absorption bands here. Thus, this region is an important contributor to the outgoing longwave radiation that ultimately leaves the Earth system. However, ozone's infrared absorption line lies within this window and so increases in ozone concentration can capture wavelengths of light that normally go relatively unabsorbed. For instance, consider a theoretical greenhouse gas that has an absorption line at 6 μm, which aligns with wavelengths that H2O strongly absorbs. As Fig. 2 shows, H2O absorbs 100% of light at this wavelength. Since H2O has completely saturated the absorption of this wavelength, changing the concentration of this theoretical molecule would not have an impact on Earth's greenhouse effect. However, for ozone, there is an ample supply of potential light that can still be absorbed.

2   Methods

In order to study the effect of stratospheric ozone concentration on a climate that is both realistic and simple, we chose to use an aquaplanet model configuration. An aquaplanet simulation is an idealized global atmospheric model that is completely water-covered with no land, topography, or sea ice. Aquaplanets use a data ocean, an ocean model that uses data to

force and determine its state. In the Community Earth System Model (CESM), data-oceans come in two forms: a pure data model based an prescribed sea surface temperatures (SSTs) or a slab-ocean model where bottom heat flux and boundary layer depths are supplied to update SSTs based on atmosphere-ocean fluxes. Additionally, while aquaplanets maintain a diurnal cycle, a perpetual equinox with a perfectly circular orbit (eccentricity and obliquity of zero) is enforced, resulting in no seasonal cycle. Aquaplanets provide a bridge in the hierarchy of atmospheric general circulation models between simplified physics component sets like the Held-Suarez configuration and Earth-like simulations used in the Atmospheric Modeling Intercomparison Project (AMIP).
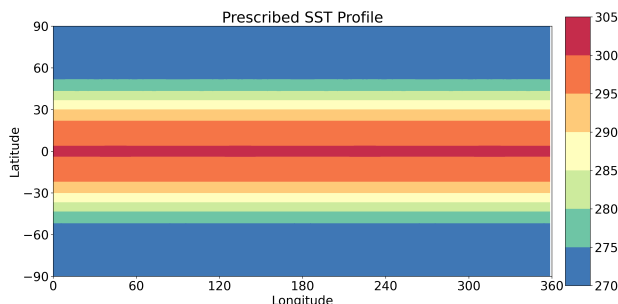

Figure 3: Prescribed sea surface temperature profile used for aquaplanet simulations.

We used the prescribed SST aquaplanet configuration in the CESM on Community Atmosphere Model, Version 4 (CAM4) due to its simplicity, low computational cost, and the fact that it can be run essentially "out-of-the-box." This model configuration is referred to as the QPC4 atmospheric component set (compset) where "Q" stands for aquaplanet, "P" for prescribed SSTs, and "4" for CAM4 physics. The aquaplanet configuration and a reference climatology on CAM5 physics is described by Medeiros et al. (2016). The CESM configuration is based primarily on the AquaPlanet Experiment Project (APE) which provide a benchmark and standard input parameters (physical constants, greenhouse gas concentrations, etc.) for aquaplanet configurations (David et al., 2012).

A powerful feature of aquaplanet configurations in CESM is that they run the full CAM parametrization suite. We opted to use the CAM4 physics suite, the simplest set available on CESM. A full description of the CAM4 suite including the spectral element dynamical core formulation and the methods used to calculate variables like cloud fraction is explained in detail in Neale et al. (2010). We note that CAM5 and CAM6 add more complexity to the available array of physical parameterizations, particularly in convection and microphysics that have significant improvements in the representations of clouds and aerosols compared to CAM4 (Reed et al., 2021).

For this project, three 10 year long simulations were conducted, each with a different input prescribed ozone concentration. One simulation is a control ozone run (1×O3) that uses the ozone distribution applied in the APE. In order to observe how increases and decreases to ozone impact climate, the other two runs apply a 4× and 1/4× factor to the 1×O3 control run respectively. Each simulation uses a spectral element dynamical core with 1° horizontal resolution and a 72 vertical level resolution with a 0.1 hPa ($\sim$ 60 km) model top over the course of 10 years. Analytical moist baroclinic wave initial conditions are supplied. The

zonally-uniform, time-independent prescribed SST and ozone distribution used in the model are given in Fig. 3 and Fig. 1 respectively. Since a "spin-up" analysis was not conducted to ensure simulation convergence to a stable climate state, all time averages conservatively used only the last 5 years. Medeiros et al. (2016) indicate spin-up is achieved by around 3 months and robust zonal-mean structure converges by two years. Due to the limited time for this project, the analysis of ozone's influence on climate will be primarily qualitative with the support of plots and simple balances that hold in the atmosphere.

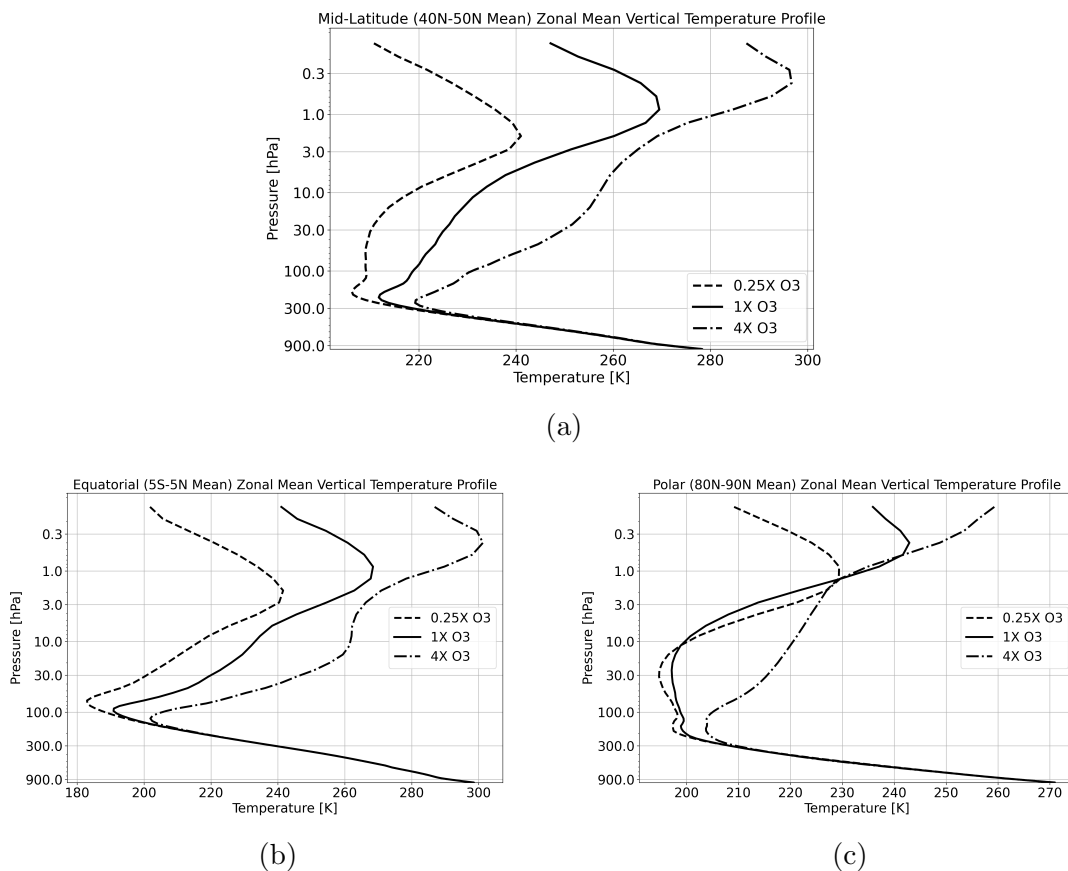# 3   Discussion

3.1   Temperature

(a)

(b)

(c)

Figure 4: Characteristic temperature profiles for each ozone simulation averaged over (a) the mid-latitudes $(40°N - 50°N)$, (b) the tropics $(5°S - 5°N)$, and (c) the polar region $(80°N - 90°N)$. Each profile is a 5-year zonal mean.

First, we will overview how vertical temperature profiles differ in the 4×O3 and 1/4×O3 runs compared to the 1×O3 control. To obtain characteristic temperature profiles for the tropics, mid-latitude, and polar regions, we compute area-weighted meridional averages over $5°S - 5°N$, $40°N - 50°N$, and $80°N - 90°N$ latitudinal bands. Due to the zonally-uniform

nature of the model inputs, there is no appreciable difference between the mid-latitude and polar regions between the Northern and Southern hemispheres. Then, for each profile, a 5-year zonal average is calculated to obtain a characteristic pressure-temperature profile, shown in Fig. 4a-4c.

In response to greater 4×O3, Fig. 4a-4c shows that stratospheric temperatures increase at nearly all levels, particularly most prominent near the middle of the stratosphere where ozone is most concentrated. Generally, the temperature of the tropopause and stratopause increase, while the troposphere otherwise remains at the same temperatures with an unchanged lapse rate. Under a hydrostatically balanced atmosphere, the hyposmetric equation (Eq. 1) can be used to understand how the changing pressure levels and temperatures of the stratosphere relate to changes in the thickness. The overall increase in stratospheric temperatures, which increase the layer-mean temperature T, and the changes in the stratopause and tropopause heights ultimately produce a significantly thicker stratosphere. The reduction in tropopause pressure and temperature have the opposite effect in the 1/4×O3 simulation, resulting in a thinner stratosphere.

$$\Delta Z = \frac{R_d T}{g} \ln \left(\frac{p_{\text{low}}}{p_{\text{high}}} \right) \tag{1}$$

In the 1/4×O3 run, the opposite occurs. An overall cooler, narrower stratosphere is present with a cooler tropopause. The tropospheric lapse rate remains constant here as well. These results align with the expectations from ozone's radiative properties. More ozone results in greater solar absorption and long wave absorption in the atmospheric window that cause stratospheric ozone.

The polar temperature profile, where ozone is most sparse, is particularly distinct from the mid-latitude and tropical temperature profiles. The increase of the stratopause level in the 4×O3 is the most extreme and extends past the model top. Furthermore, while the 1×O3 and 1/4×O3 have a large region of nearly uniform temperatures above the tropopause between 100hPa and 20 hPa , the 4×O3 run has a more unambiguous flip in its lapse rate similar to all the temperature profiles in the mid-latitudes and tropics. This may suggest a critical concentration of ozone at which a sharp tropopause transition to the stably stratified stratosphere occurs.

3.2 Atmospheric Circulation

Next, we see how ozone concentrations influence the general atmospheric circulation on the aquaplanet. Fig. 5 shows the 5-year zonal average of the zonal velocity in 1×O3 control and difference plots of 4×O3 and 1/4×O3 with respect to the control. At higher ozone levels, the polar stratospheric jets increase in strength on order of $20 - 30$m/s while the tropospheric subtropical jets weaken slightly, on order of 10 m/s. The opposite is observed with the lower ozone levels, with a weakening of stratospheric jets on order of $40-60$ m/s and strengthening of tropospheric jets by $10 - 15$ m/s.

Figures 6a-6c and 6d-6f depict the 5-year zonal average of the horizontal and vertical branches of the Hadley Cell circulation in the tropics respectively for the control 1×O3 and the differences of 4×O3 and 1/4×O3 with respect to the control. Fig. 6e displays a weakening of the top and bottom of the Hadley circulation branches for greater ozone concentrations,
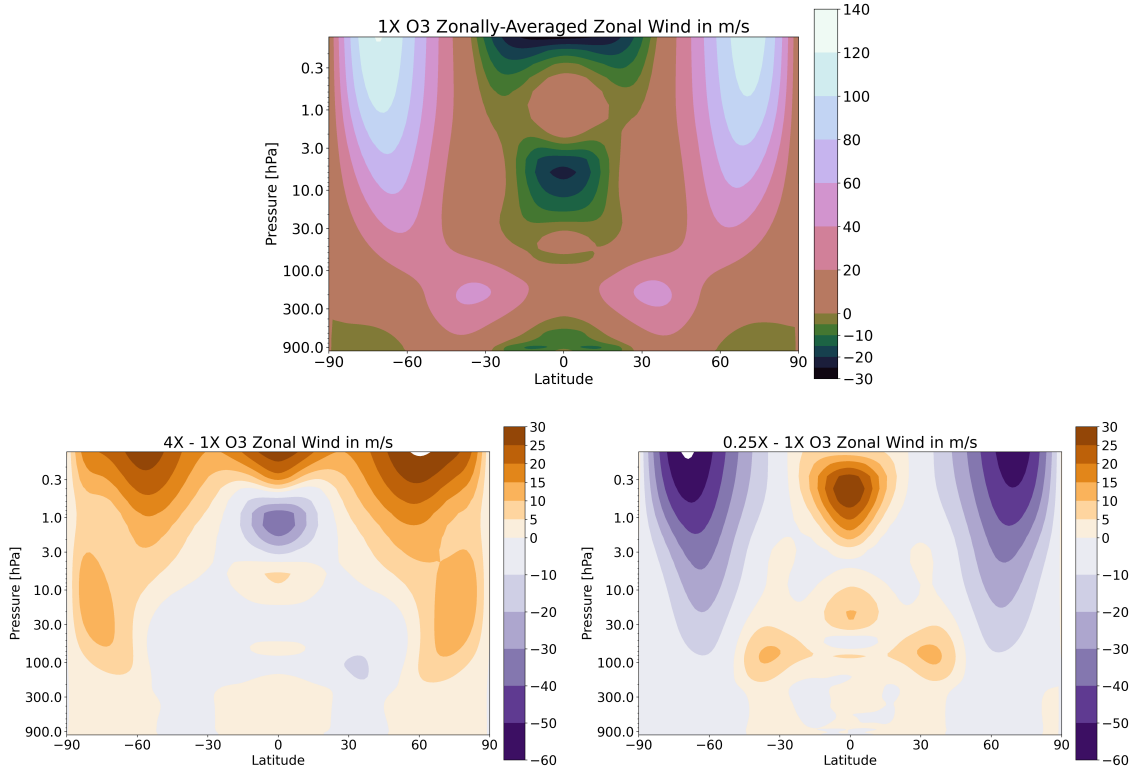
Figure 5: Zonal wind for 1×O3 (top) and difference plots: 4×O3−1×O3 (left) and 1/4×O3−1×O3 (right). The plotted zonal wind for each simulation are 5-year, zonal averages.

with a more prominent weakening at the tropopause. In the free atmosphere, omega, the vertical velocity in pressure coordinates, is proportional to the negative vertical velocity in height coordinates. Thus, it can give a measure of the ascending and descending motions of air. In Fig. 6a, the control has overall negative omega at the equator (ascending air) and positive omega at the subtropics (descending air). The difference plots show a relatively large weakening in the ascending and descending branches for 4×O3 and a relatively small strengthening for 1/4×O3.

3.3 Energy Balance

In a realistic model, the surface temperatures would respond and change in response to changes in greenhouse gases, such as the increase in surface temperatures we currently observe due to anthropogenic CO2 emissions. For the aquaplanet, the external forcing by the Sun and the fixed SST distribution hold the input radiative flux and surface radiative flux constant. Thus the changes we observe in these simulations reflect how an atmosphere under fixed top and bottom radiative fluxes would respond to changes in ozone. This is, importantly, distinct from how Earth's climate system would change in response to the same ozone changes because Earth's atmosphere has **only** an approximately fixed (on long decadal time scales) **top** of atmosphere input from the Sun. Thus the simulations may not realistically
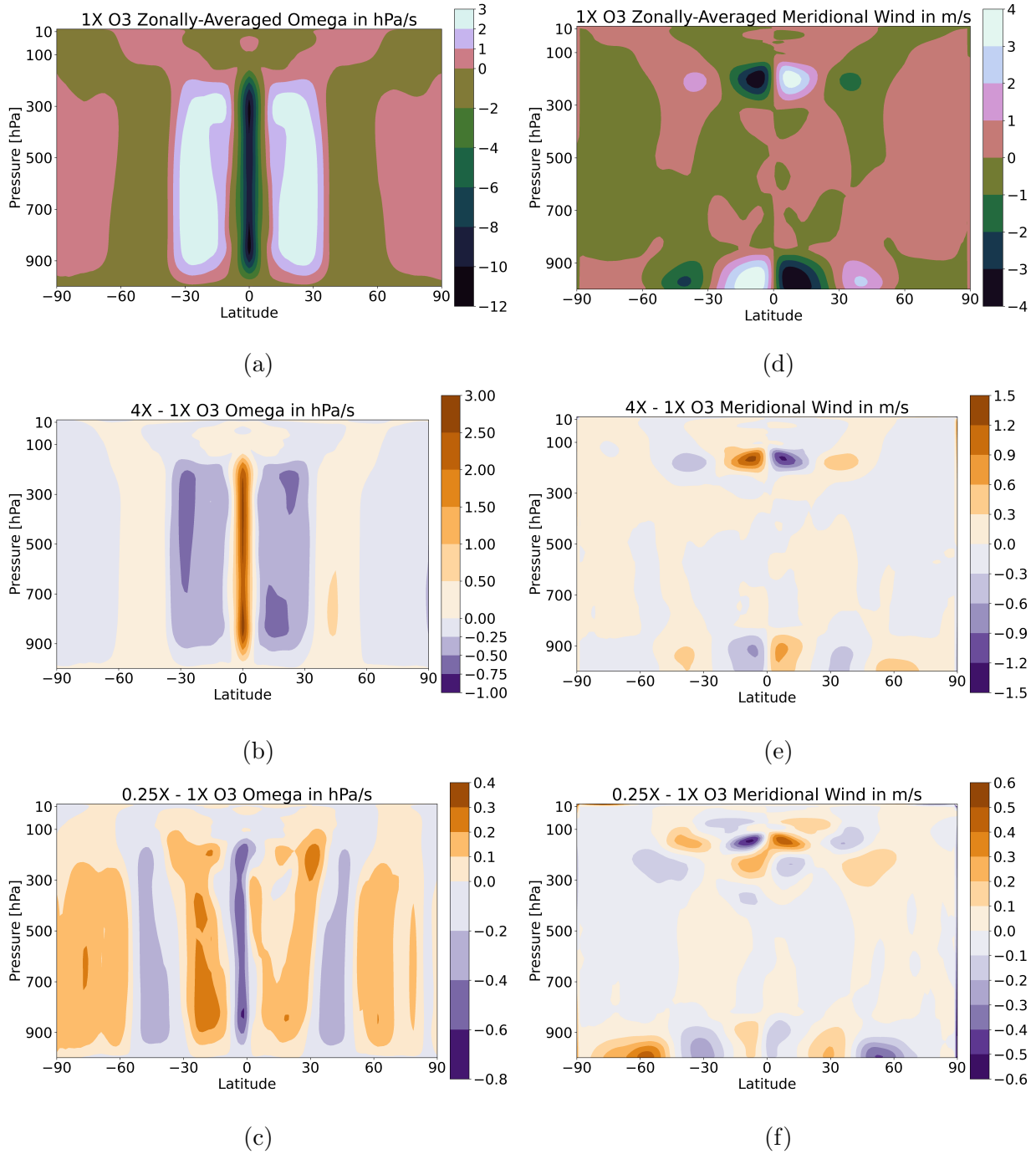
Figure 6: **Left Column**: Omega vertical velocity for 1×O3 (a) and difference plots: 4×O3−1×O3 (b) and 1/4×O3−1×O3 (c). The plotted values for each simulation are all 5-year, zonal averages. **Right Column**: Meridional wind for 1×O3 (d) and difference plots: 4×O3−1×O3 (e) and 1/4×O3−1×O3 (f).

depict how changes in ozone would change the radiative-convective balance near the surface on Earth.
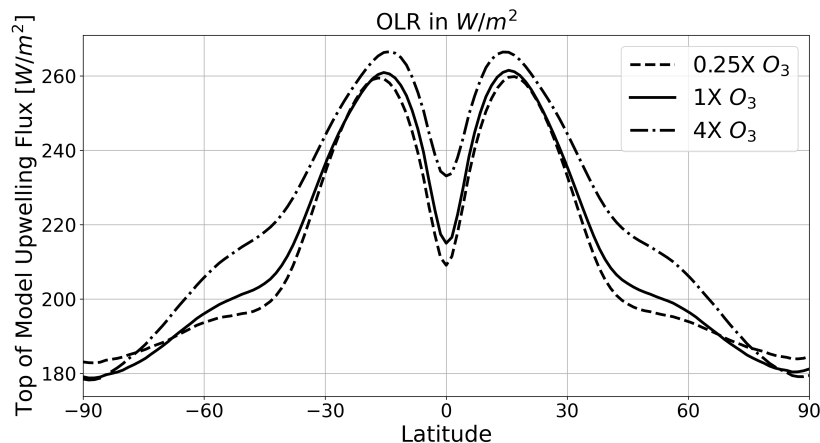

Figure 7: The 5-year, zonal average of the top-of-model upwelling longwave flux, a measure of the outgoing longwave radiation for each simulation,

The top-of-atmosphere (TOA) global energy balance is a balance between the total absorbed solar radiation, which is dependent on the planetary albedo, and the outgoing longwave (LW) radiation (OLR) that leaves the Earth system. For a stable climate system, the imbalance of solar absorption and OLR is approximately zero. So if a difference in OLR is observed between the ozone simulations, this implies a change in the global solar absorption, a function of only the planetary albedo. In Fig. 7, the 5-year zonally averaged, top-of-model upwelling LW flux is plotted for all three simulations. This variable is a measure of the OLR for the model atmosphere that only extends up to around 60 km. Fig. 7 shows that as ozone concentration increases, the OLR increases in the tropical and subtropical regions. In polar regions (above $\pm 75°$ latitude), the relationship is not clear cut and instead OLR becomes the largest for the $1/4 \times O3$ run. This may explain why the polar temperature profiles are characteristically different from profiles in the tropics and subtropics.

The Stefan-Boltzmann radiation law indicates that an increase in stratospheric temperatures from increased radiative absorption by ozone, would increase the LW heating rate of the stratosphere resulting in a larger overall OLR. In response to the greater OLR, we should then expect the planetary albedo to decrease in order to maintain the TOA balance indicative of a stable climate. Since an aquaplanet is without land, sea-ice, or biological influences, the primary variable that can cause changes in the planetary albedo is the amount of cloud cover. Fig. 8 gives the 5-year zonally and vertically averaged cloud fraction for each simulation. It can be seen that in the tropics, the average cloud fraction decreases at higher ozone concentration while in the polar region, cloud fraction increases. In general, the albedo of clouds, is larger than the albedo of the ocean (Hartmann, 2016a). So if the global average cloud cover decreases, the planetary albedo decreases causing greater solar absorption. Thus, cloud cover plays a role in offsetting the greater OLR observed at higher ozone concentrations.

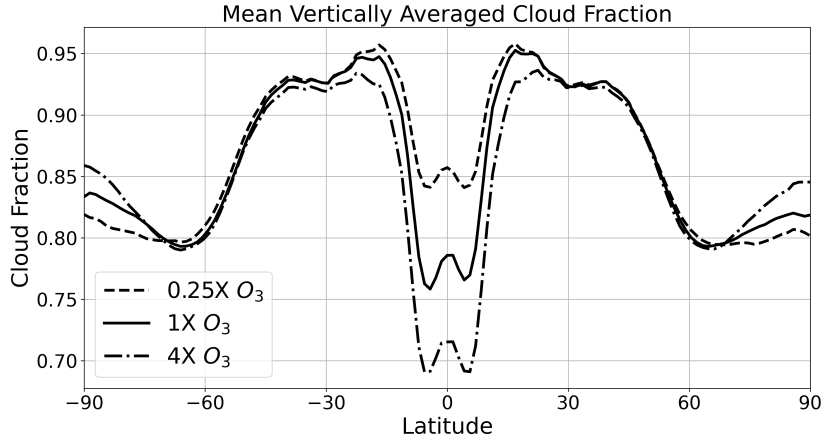However, clouds are made up of water, the most prominent greenhouse gas on Earth.

Figure 8: The 5-year, zonal mean of the vertically averaged cloud fraction.

In addition to the albedo radiative effect due to clouds, clouds also have a LW radiative effect based upon their altitude (Hartmann, 2016b). Higher clouds in the troposphere emit LW radiation at cooler temperatures and therefore emit at a smaller rate based on the Stefan-Boltzmann law. Ultimately, the LW radiative effect from clouds could influence the OLR. Looking at the 5-year, zonally averaged tropical cloud fraction profile with height in Fig. 9, the pressure level of low $(1000 - 700$ hPa), mid $(700 - 400$ hPa), and high clouds $(400 - 0.1$hPa$)$ is relatively unchanged for 4×O3 compared to the control, indicated that the dominant difference in cloud radiative effect in the tropics for these two simulations is the albedo effect. On the other hand, while no change in low and mid level clouds is observed for the 1/4×O3 run, there is an increased presence of high clouds at 100 hPa while there is little difference in the ~ 250 hPa peak of high top clouds. The presence of higher altitude clouds has a warming effect on the tropical energy balance that offsets some of the cooling effect caused by the increased vertical averaged tropical cloud cover.

Finally, we can explore the radiative balance of LW and shortwave (SW) radiation throughout the atmosphere by the LW and SW radiative heating rates. Fig. 10 depicts the LW, SW, and net (LW+SW) radiative heating rates for each simulation for the stratosphere and the troposphere. Overall, the shape of the net radiative heating rates in the troposphere and stratosphere remain unchanged. The approximately net zero radiative heating rates in the stratosphere is indicative that the stratosphere is in radiative equilibrium, while the net cooling in the troposphere implies it is not in radiative equilibrium as expected. The troposphere is in a radiative-convective balance where it radiatively cools to offset the heat exchange by convective processes from the surface that is warmed by the Sun. The radiative heating profiles for each simulation indicates that the tropospheric LW and SW heating rates are relatively independent of the ozone concentration. On the other hand, the LW and SW heating rates in the stratosphere are highly correlated with the ozone concentration as expected. At greater ozone concentrations, solar absorption increases resulting in higher stratospheric temperatures that increase the LW heating rate. This continues until a radiative balance is attained.
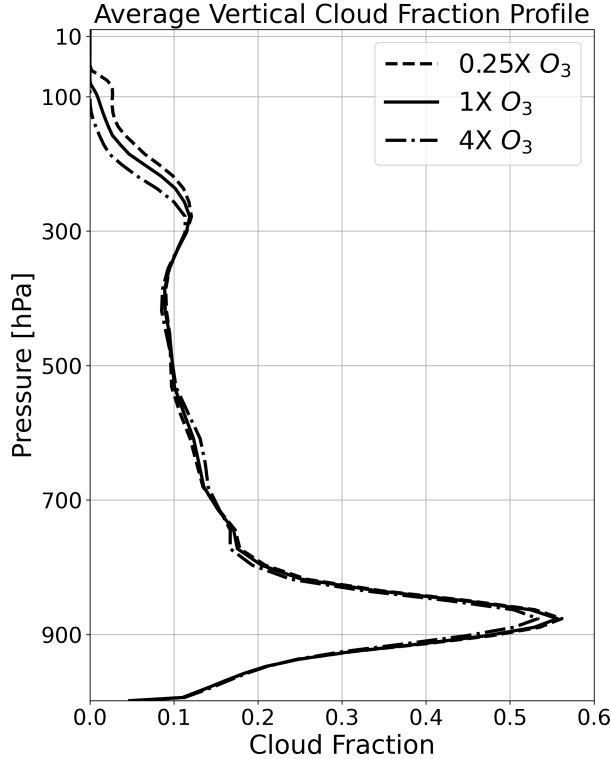
9

Figure 9: The cloud fraction profile with pressure, computed with a 5-year, zonal and area-weighted meridional mean of cloud fraction.

3.4 Quasi-Biennial Oscillation

While the focus of this project has primarily been on how climatological, zonally averaged quantities have changed in response to ozone, ozone concentration can also influence oscillations in the general atmospheric circulation. One such oscillation, is the quasi-biennial oscillation (QBO) in the stratosphere. The QBO is an oscillation in the prevailing tropical stratospheric zonal winds. The QBO has an easterly and a westerly phase. The phases are asymmetric in the sense that the easterly phase is larger in amplitude (wind speed). Each QBO phase begins at the top of the stratosphere, with the new prevailing wind spreading downwards until it hits the tropopause. To obtain the QBO in the aquaplanet simulations, we adjusted the CAM4 configuration to enable gravity wave production by frontogenesis and deep convection, which are necessary in driving the QBO. The QBO for the control aquaplanet can be seen in Fig. 11, which is similar in structure to the QBO observed on Earth.

Fig. 12 shows the QBO calculated for the 4×O3 and 1/4×O3 simulations. At lower ozone concentrations, the QBO period becomes shorter and the increase in tropopause height can be observed by the rise in the band of westerly winds around 100 hPa. At higher ozone concentrations, the QBO period is extended and more asymmetric with longer easterly phases compared to shorter and weaker westerly phases
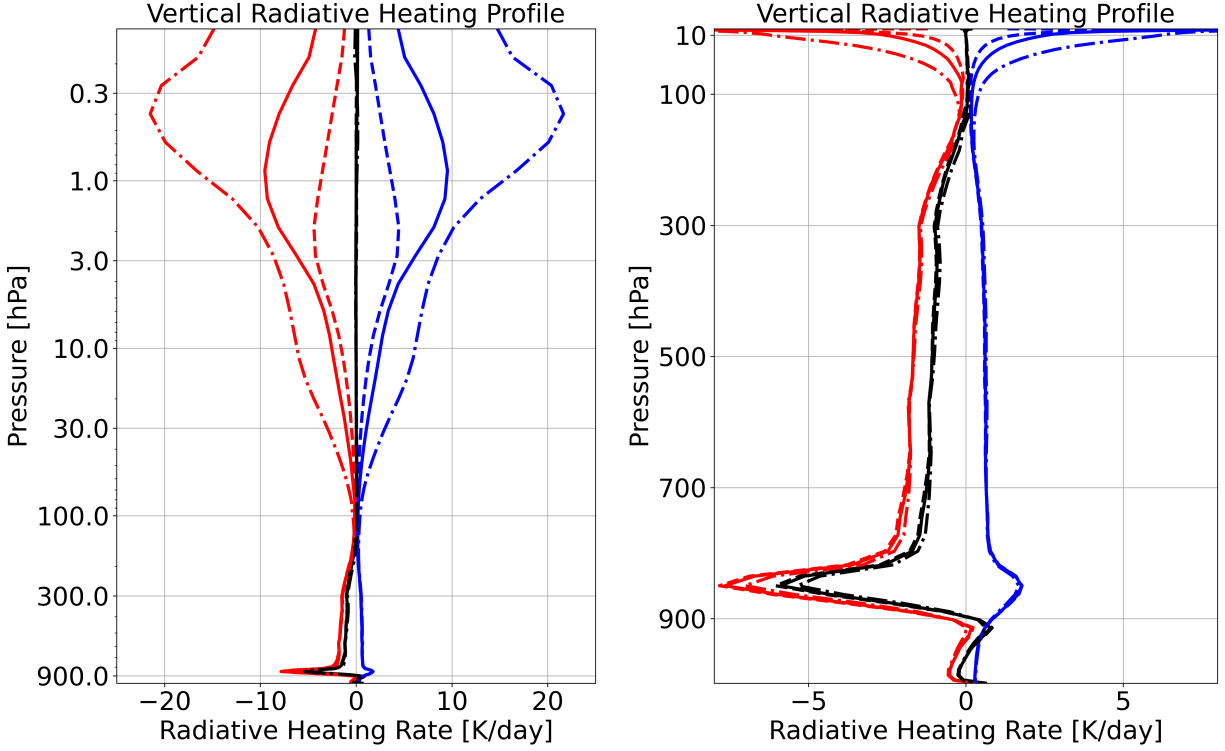
10

Figure 10: The 5-year zonal and area-weighted meridional mean radiative heating rate profile for LW heating (red), SW heating (blue), and net heating (LW+SW) for each simulation run: 1×O3 (solid), 4×O3 (dash-dot), and 1/4×O3 (dash-dash). The profile is plotted with a log-pressure scale (left) to focus on the stratosphere and a linear-pressure scale (right) to focus on the troposphere.

4   Conclusion

In an idealized, fixed SST aquaplanet configuration, changes in the ozone concentration have significant impacts on the general atmospheric circulation despite the fact that surface temperatures remain the same. At higher ozone concentrations, the stratosphere thickens, raising the stratopause and depressing the tropopause height. Polar stratospheric jets are strengthened while the subtropical jets and the Hadley circulation are weakened. The global OLR increases while the global vertically averaged cloud fraction decreases, particularly at the tropics, implying a decrease in the planetary albedo. Moreover, the QBO period lengthens in response to greater ozone concentrations. The opposite effects are observed at lower ozone concentrations. These changes depict how climate states are not uniquely characterized by their surface temperatures. Even at the same surface temperature, the general atmospheric circulation can behave differently based upon the stratospheric distribution of ozone.

Due to the short time frame for the project, the scope of this analysis is limited. There are several interesting questions that these results bring up. It is particularly intriguing how insensitive the tropospheric lapse rate and energy balance is at different ozone concentrations. In realistic atmosphere, where surface temperatures are allowed to change, an increased
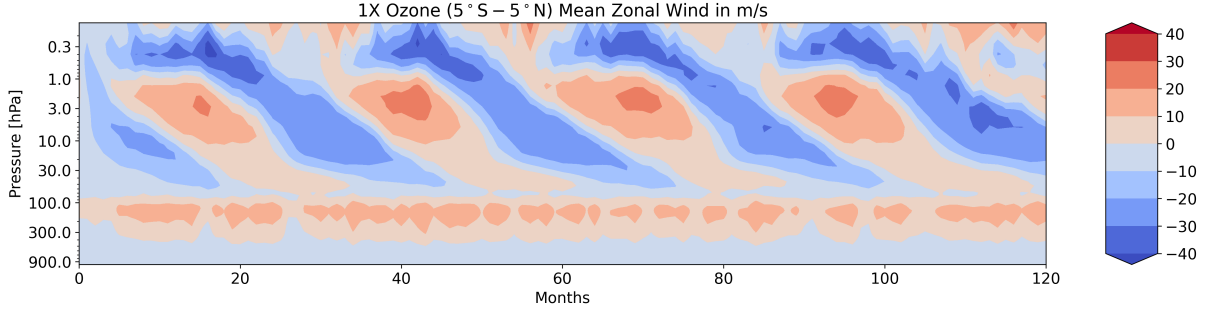
Figure 11: The area-weighted meridional mean zonal wind over the tropics $(5°S - 5°N)$ for $1\times$O3 averaged zonally over 5-years.
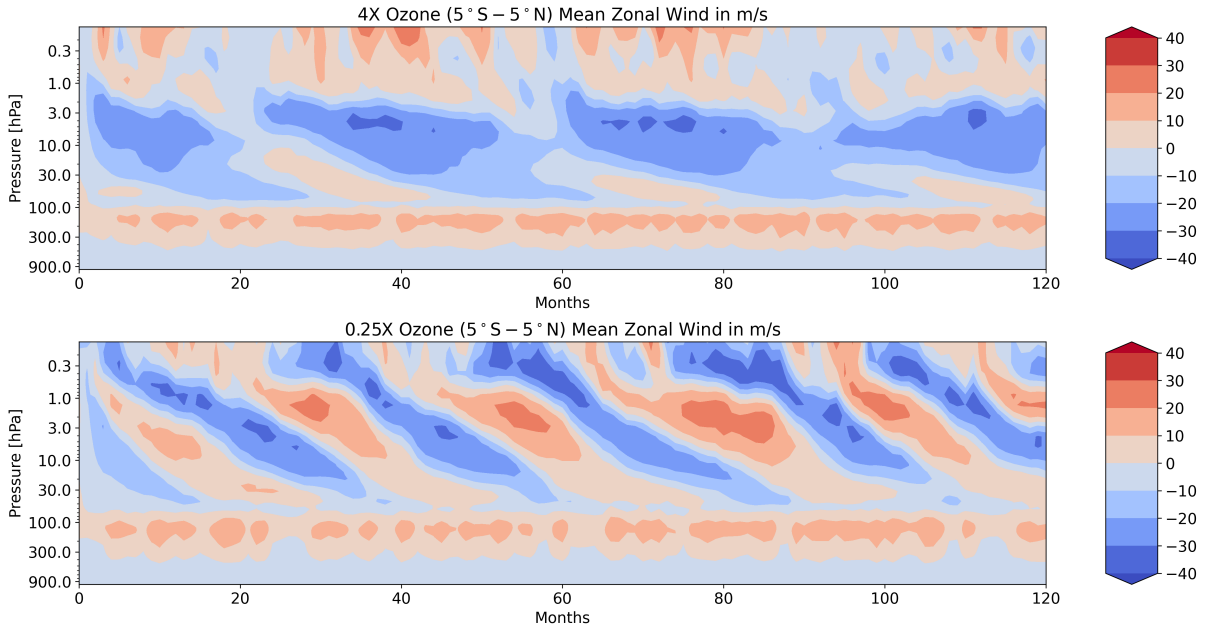

Figure 12: The area-weighted meridional mean zonal wind over the tropics $(5°S - 5°N)$ for $4\times$O3 (top) and $1/4\times$O3 (bottom) averaged zonally over 5-years.

greenhouse effect (such as by increasing ozone) would increase surface temperatures and also have an influence on the lapse rate through changes on the atmospheric moisture content. Is the forcing of SSTs that prevents changes in surface temperature also inhibiting changes in the lower tropospheric lapse rate? Another interesting question lies in the asymmetry observed between the polar response and the subtropical/tropical response to changing ozone concentrations. Is the polar asymmetry a necessary result to ensure poleward transport of energy with latitudinally-varying ozone and SST distributions that peak in the tropics? Another area of further study is in the exploration of what other variables influence the tropopause height besides ozone. Finally, the analysis of cloud properties in this paper only scratched the surface. On an aquaplanet, it is clear that clouds are important in controlling the planetary albedo and influencing the LW radiative balance. Conducting a more thorough analysis on the complex properties of clouds on the aquaplanet system could reveal interesting feedbacks between the stratospheric radiative balance and tropospheric clouds, particularly

those near the tropopause.

References

David, L. W., Blackburn, M., Brian, J. H., and Nakajima, K. (2012). The APE atlas. *NCAR Technical Report*, page 31354.

Hartmann, D. L. (2016a). Chapter 2 - the global energy balance. In Hartmann, D. L., editor, *Global Physical Climatology (Second Edition)*, pages 25–48. Elsevier, Boston, second edition edition.

Hartmann, D. L. (2016b). Chapter 3 - atmospheric radiative transfer and climate. In Hartmann, D. L., editor, *Global Physical Climatology (Second Edition)*, pages 49–94. Elsevier, Boston, second edition edition.

Medeiros, B., Williamson, D. L., and Olson, J. G. (2016). Reference Aquaplanet Climate in the Community Atmosphere Model, Version 5. *Journal of Advances in Modeling Earth Systems*, 8(1):406–424.

Neale, R. B., Richter, J. H., Conley, A. J., Park, S., Lauritzen, P. H., Gettelman, A., Williamson, D. L., Rasch, P. J. R., Vavrus, S. J., Taylor, M. A., Collins, W. D., Zhang, M., and Lin, S.-J. (2010). Description of the NCAR Community Atmosphere Model (CAM 4.0). *NCAR Technical Report*, (485):224.

Reed, K. A., Silvers, L. G., Wing, A. A., Hu, I.-K., and Medeiros, B. (2021). Using Radiative Convective Equilibrium to Explore Clouds and Climate in the Community Atmosphere Model. *Journal of Advances in Modeling Earth Systems*, 13(12):e2021MS002539. e2021MS002539 2021MS002539.

Smith, R. S., Dubois, C., and Marotzke, J. (2006). Global Climate and Ocean Circulation on an Aquaplanet Ocean–Atmosphere General Circulation Model. *Journal of Climate*, 19(18):4719 – 4737.

Valley, S. L. (1965). Handbook of Geophysics and Space Environments. Interim report.

5   Appendix: Ocean Gyres on Aquaplanets

In class, we briefly discussed whether or not a planet without land, like an aquaplanet, would have ocean gyres. With a prescribed SST data-ocean, this question cannot be studied by the simulations run for this project as there is no explicit modeling of the ocean circulation. However, this analysis is possible for slab-ocean aquaplanet models. The authors Smith et al. (2006) conducted a study that addresses this very question. In the study, they conducted three coupled ocean-atmosphere slab-ocean aquaplanet-like experiments on a low-resolution version of the Fast Ocean, Rapid Troposphere Experiment (FORTE) model. The first configuration was a typical aquaplanet (WaterWorld) with no land or topography, the second an
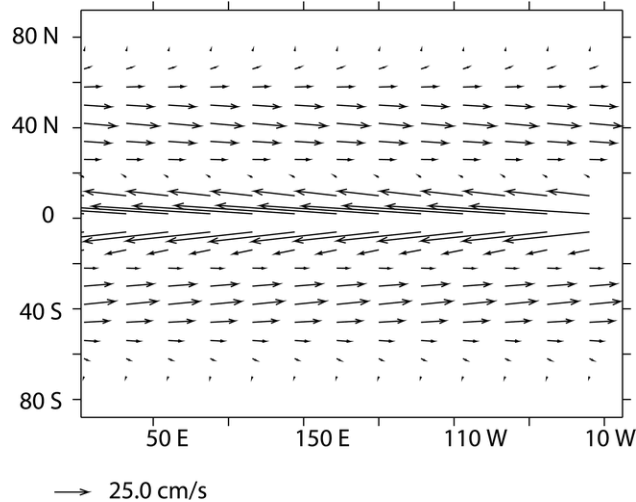
Figure 13: Annual average sea surface currents in cm s^{-1} on WaterWorld. Figure from Smith et al. (2006).

aquaplanet that contained a low barrier that blocks zonal flow in the ocean at all latitudes (RidgeWorld),and third an aquaplanet with a meridional barrier with a gap in the Southern hemisphere that allows circumglobal flow (DrakeWorld).

In the WaterWorld, there are no ocean basins, just a single global ocean. The observed surface currents, depicted in Fig. 13, are predominantly zonal wind-driven currents, which without land are determined primarily by the friction within the ocean and at the ocean floor. While no ocean gyres occur on the WaterWorld, the same Ekman transport patterns exist. Figure (a) in Fig. 14 gives the meridional overturning streamfunctions in Sverdrups, where positive (darker) values indicate clockwise flow. At the tropics, there is an overall divergence at the surface and convergence in the deep ocean that produces Ekman suction and Ekman transport poleward. At the subtropics $\left(\text{around } \pm(20° - 30°)\right)$ there is convergence and Ekman pumping that brings cold polar waters equatorward, resulting in overall poleward energy transport.

Now, when an orographic barrier is introduced to create an ocean basin, the ocean gyres emerge. Fig. 15 gives the horizontal streamfunctions in Sverdrups where positive (darker) values indicate clockwise flow. The RidgeWorld develops one global ocean basin with 4 gyre structures that behave similar to the subtropical (clockwise in the Northern hemisphere) and subpolar (counterclockwise in the Northern hemisphere) gyres observed on Earth. On the other hand, the southern gap in DrakeWorld produces an analogue to the westward flow of the Antarctic circumpolar current on Earth.
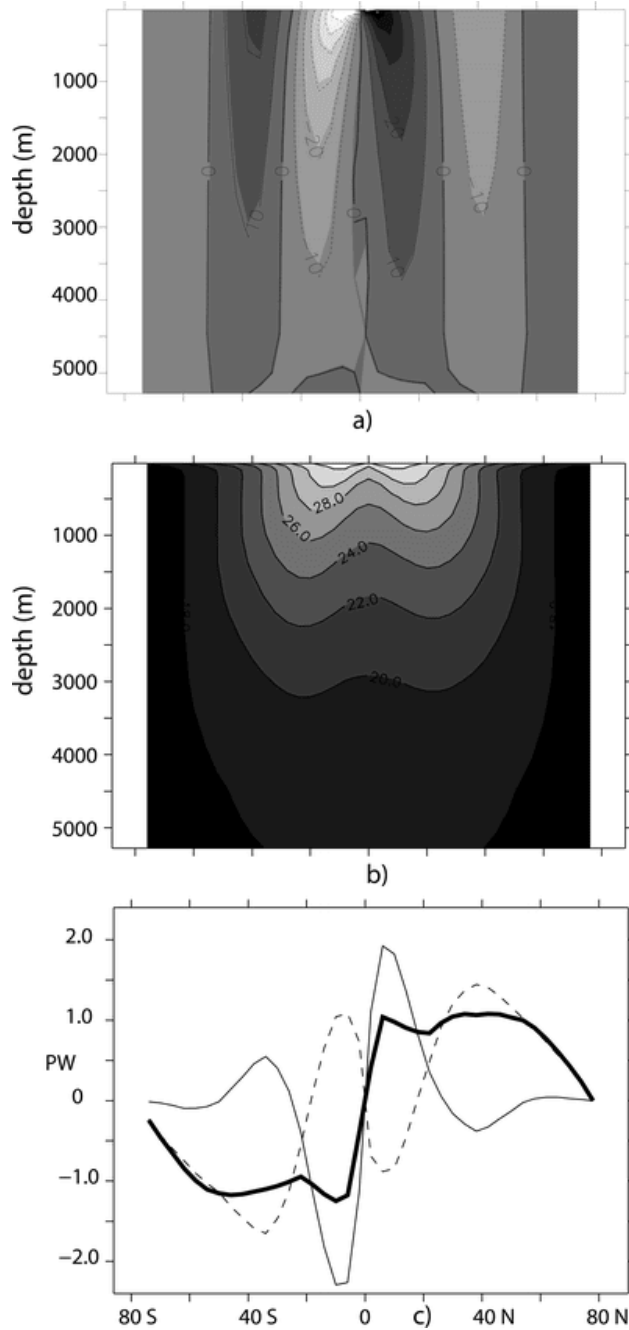
Figure 14: The WaterWorld (a) meridional overturning streamfunction in Sverdrups where positive is clockwise flow, (b) annually, zonally averaged temperature with depth in $^{\circ}C$, and (c) the oceanic poleward transport of heat split into advective (light), nonadvective (dashed), and total (heavy) contributions. Figure from Smith et al. (2006).
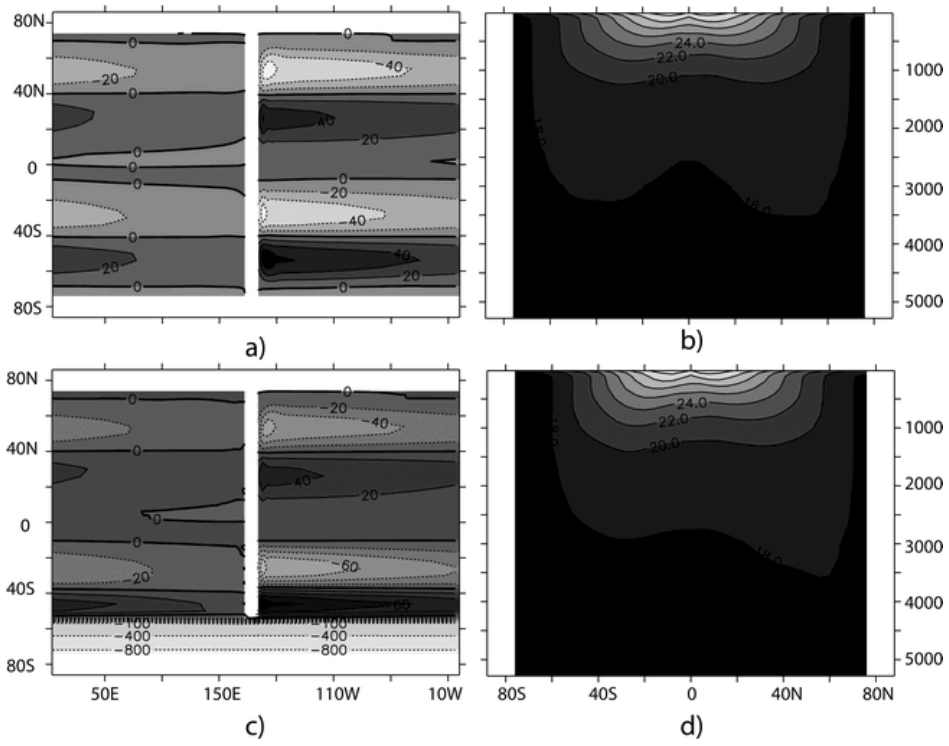
15

Figure 15: **Left Column**: Horizontal streamfunctions in Sverdrups (positive is clockwise flow) for (a) RidgeWorld and (c) DrakeWorld. The region of no flow around 180E is due to the orographic boundaries present in each system. **Right Column**: Zonally averaged temperature with depth in °C for (b) RidgeWorld and (d) DrakeWorld Figure from Smith et al. (2006).